SPINE Volume 29, Number 9, pp 979–987

Soft Tissue Injury Threshold During Simulated Whiplash

A Biomechanical Investigation

Shigeki Ito, MD,*† Paul C. Ivancic, MPhil,* Manohar M. Panjabi, PhD,* and Bryan W. Cunningham, MSc‡

Study Design. A newly developed biofidelic whole cervical spine (WCS) model with muscle force replication (MFR) was subjected to whiplash simulations of varying intensity, and the resulting injuries were evaluated through changes in the intervertebral flexibility.

Objectives. To identify the soft tissue injury threshold based on the peak T1 horizontal acceleration and the association between acceleration magnitude and injury severity resulting from simulated whiplash using the WCS + MFR model.

Summary of Background Data. Whiplash has been simulated using mathematical models, whole cadavers, volunteers, and WCSs. The measurement of injury (difference between prewhiplash and postwhiplash flexibilities) is possible only using the WCS model.

Methods. Six WCS + MFR specimens (C0–T1) were incrementally rear-impacted at nominal T1 horizontal maximum accelerations of 3.5, 5, 6.5, and 8 *g*, and the changes in the intervertebral flexibility parameters of neutral zone and range of motion were determined. The injury threshold acceleration was the lowest T1 horizontal peak acceleration that caused a significant increase in the intervertebral flexibility.

Results. The first significant increase ($P < 0.01$) of 39.8% occurred in the C5–C6 extension neutral zone following the 5 *g* acceleration. At higher accelerations, the injuries spread among the surrounding levels (C4–C5 to C7–T1).

Conclusions. A rear-end collision is most likely to injure the lower cervical spine by intervertebral hyperextension at a peak T1 horizontal acceleration of 5 *g* and above. These results may aid in the design of injury prevention systems and more precise diagnoses of whiplash injuries. [Key words: whiplash, biomechanics, spinal instability, cervical spine, injury threshold] **Spine 2004;29:979–987**

Acute neck pain following low speed rear-end collisions is common; however, controversy exists regarding the causes of chronic pain following whiplash. Several hypotheses exist to explain the basis of chronic neck pain including injury to the facet joints,[1–5] intervertebral disc,[6,7] spinal ligaments, and spinal ganglions[8–10] in addition to psychosocial factors.[11–14] The facet joint injury hypothesis has been supported by numerous clinical observations.[15–20]

There exist a wide variety of approaches to study whiplash injuries, including mathematical models[21,22] and whiplash simulation of entire cadavers on sleds[2,23] and isolated whole cervical spine (WCS) specimens on mini-sleds.[1,24–30] Although human volunteers within sleds or automobiles have been rear-impacted to obtain kinematic data of the head and cervical spine, the *in vivo* whiplash simulations must be performed below the injury threshold.[5,31–39] Of the previous approaches, only the WCS model is capable of quantifying the soft tissue injuries, *via* prewhiplash and postwhiplash flexibility tests. Using the WCS model and the incremental trauma approach, Panjabi *et al*[27] found that the lower intervertebral levels were prone to injury during low-energy rear impacts, while both the upper and lower cervical spine regions were potential injury sites as the impact acceleration increased. The observed disruptions of the anterior longitudinal ligament and anterior disc at C5–C6 were consistent with increases in C5–C6 flexibility parameters and also with clinical observations. The main limitation of the WCS model was the lack of muscle force simulation.[27] Recently, several *in vitro* lumbar[40–44] and cervical spine[45–48] static models have been presented, which include muscle force simulation.

The goals of this study were to determine the soft tissue injury threshold and the association between the impact magnitude and the resulting injury severity, using a newly developed WCS whiplash model, which included muscle force simulation. The injuries were quantified by the increases in the intervertebral flexibility resulting from the simulated rear impacts.

Materials and Methods

Overview. We first define the soft tissue injury and the injury threshold acceleration and elucidate the various steps of the protocol (Figure 1). The WCS prepared for flexibility testing was designated as the WCS model. The WCS + MFR model prepared for whiplash simulation consisted of the WCS with muscle force replication, a C0–C2 flexion limiter, and a surrogate head. Three-dimensional flexibility testing was performed on the WCS model when intact and after the final whiplash simulation. Following 2 *g* dynamic preconditioning, the WCS + MFR model was subjected to incremental whiplash simulation. After each whiplash simulation, flexion–extension flexibility test-

From the *Biomechanics Research Laboratory, Department of Orthopaedics and Rehabilitation, Yale University School of Medicine, New Haven, CT; †Department of Orthopaedic Surgery, St. Marianna University School of Medicine, Kanagawa, Japan; and ‡Orthopaedic Biomechanics Laboratory, Union Memorial Hospital, Baltimore, MD.
Acknowledgment date: December 11, 2002. First revision date: February 17, 2003. Acceptance date: July 21, 2003.
Supported by NIH Grant 1 R01 AR45452 1A2.
The manuscript submitted does not contain information about medical device(s)/drug(s).
Federal funds were received in support of this work. No benefits in any form have been or will be received from a commercial party related directly or indirectly to the subject of this manuscript.
Address correspondence to Manohar M. Panjabi, PhD, Biomechanics Research Laboratory, Department of Orthopaedics and Rehabilitation, Yale University School of Medicine, 333 Cedar St., P.O. Box 208071, New Haven, CT 06520-8071; E-mail: manohar.panjabi@yale.edu

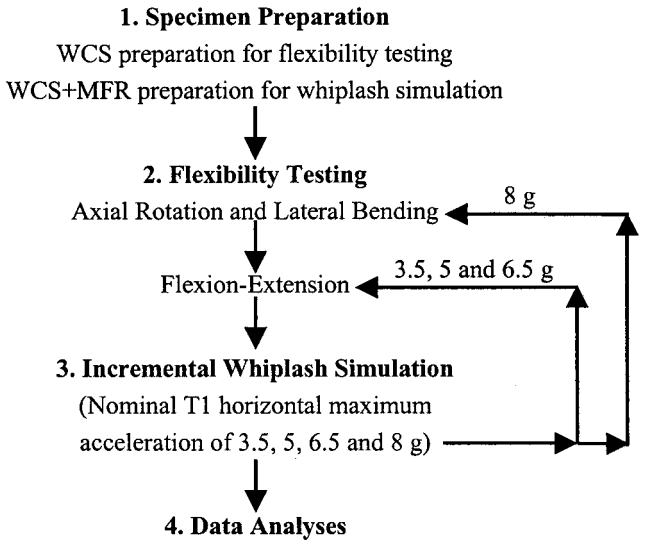

Figure 1. Experimental protocol showing various steps.

ing was performed on the WCS model without MFR to determine the injuries, if any.

Definitions of Soft Tissue Injury and the Injury Threshold Acceleration. Anatomic dissection was not performed since the subfailure soft tissue injuries that occur during whiplash are not visually identifiable. However, their functional effect in the form of increased intervertebral joint laxity may be quantified. These functional injuries are important as they may lead to accelerated joint degeneration and osteoarthritis in whiplash patients. Based on these observations, the following definition for the soft tissue injury was adopted.

Soft Tissue Injury. The soft tissue injury was defined as a significant increase ($P < 0.05$) in the intervertebral flexibility of the cervical spine resulting from simulated whiplash.

Injury Threshold Acceleration. The injury threshold acceleration was the lowest T1 horizontal peak acceleration that caused a significant increase ($P < 0.05$) in the intervertebral flexibility.

Specimen Preparation. Six fresh-frozen human cervical spine specimens consisting of the occiput through T1 were prepared by carefully dissecting all nonosteoligamentous soft tissues. There were four male and two female donors, with an average age of 70.8 years (range, 52–84 years). Apart from typical age-related changes, the donors had not had head or neck trauma and did not have any disease that could have affected the osteoligamentous structures. To prepare a specimen, the occiput and T1 were set in two parallel horizontal resin mounts (Fiber Glass-Evercoat, Cincinnati, OH). The specimen was oriented such that a line from the top of the dens to the lowest point on the posterior occiput was horizontal and the T1 vertebra was tilted anteriorly by 24°.[49] Radiography was used to verify neutral posture alignment. For attachment of motion measuring flags, headless wood screws, aligned sagittally, were drilled into the anterior aspect of each vertebral body (C2–C7) and through the left lateral mass of C1.

WCS Preparation for Flexibility Testing. To prepare a WCS for flexibility testing, a loading jig was applied to the occipital mount, while the T1 mount was fixed to the test table (Figure 2A). The weights of the loading jig and occipital mount were counterbalanced during flexibility testing.

WCS + MFR Preparation for Whiplash Simulation. The WCS and MFR were integrated with the aim of enhancing the dynamic biofidelic response to simulated whiplash (Figure 2B). Stainless steel lateral guide rods (3.0 mm diameter) were inserted into the vertebral bodies in the frontal plane through approximate centers of rotation of each intervertebral joint. Since C1 does not have a vertebral body, no rod was inserted at this level. A surrogate head with mass 3.3 kg and sagittal plane moment of inertia of 0.016 kg/m^2 was attached to the occipital mount.[50] The MFR system consisted of four anterior, two posterior, and eight lateral cables attached to preloaded 30 N springs anchored to the base. The stiffness coefficient of each spring was 4.0 N/mm. Anterior and posterior cables originated at the occipital mount, ran along pulleys within the T1 mount, and connected to the springs. Bilateral MFR cables originated from C0, C2, C4, and C6, passed along the lateral guide rods, ran along pulleys at the T1 mount and were attached to the springs. With this MFR arrangement, the compressive preloads at each intervertebral level were as follows: 120 N (C0–C1, C1–C2); 180 N (C2–C3, C3–C4); 240 N (C4–C5, C5–C6); and 300 N (C6–C7, C7–T1). In order to allow only physiologic motions of C0–C1 and C1–C2, the specimens were instrumented with a C0–C2 flexion limiter, which consisted of a wire loop connecting the occipital mount to the C2 posterior process. Throughout whiplash, the surrogate head and WCS were stabilized with compressive MFR without requiring a tensile

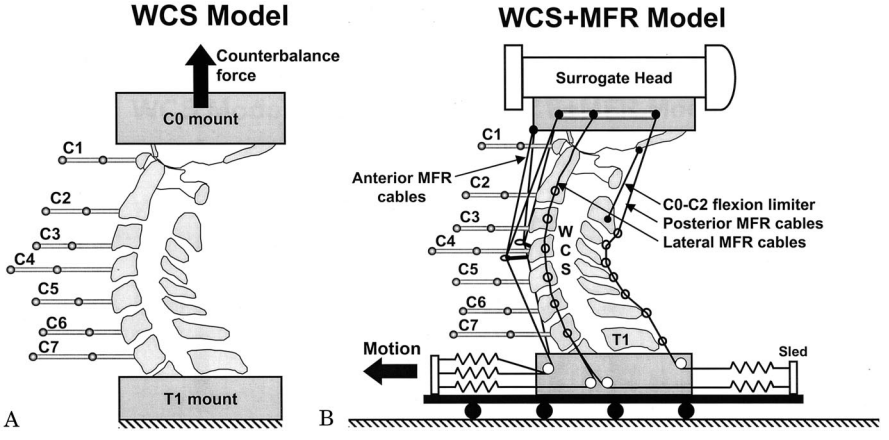

Figure 2. There were two model configurations: (**A**) whole cervical spine (WCS) for flexibility testing to determine injury and (**B**) the WCS with muscle force replication (WCS + MFR) subjected to whiplash simulation.

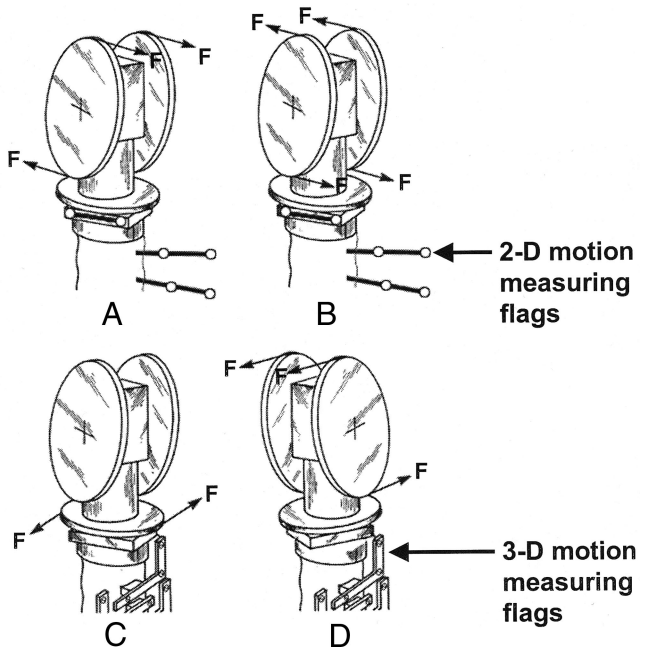

Figure 3. Flexibility testing: flexion (**A**), extension (**B**), axial rotation (**C**), and lateral bending (**D**). Two-dimensional flexion–extension testing was performed on all intact specimens, following the 2 *g* dynamic preconditioning and following each whiplash simulation. Three-dimensional flexibility testing was performed on intact specimens and following the final whiplash simulation.

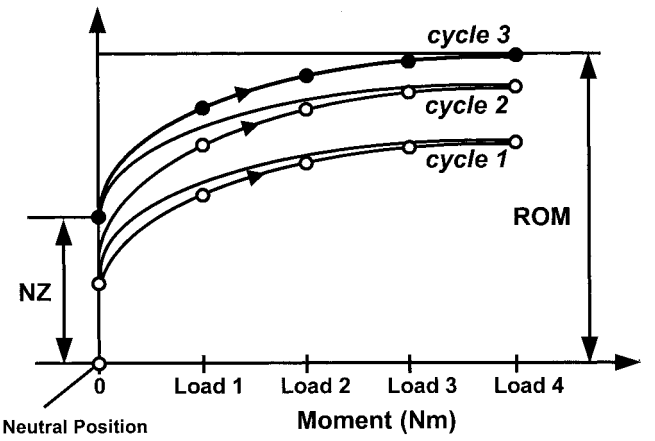

Figure 4. Flexibility testing protocol in which two preconditioning cycles were performed and data were collected on the third loading cycle. Pure moments were applied in four equal steps up to peak loads of 1.5 Nm, 3 Nm, and 1.5 Nm in flexion–extension, axial rotation, and lateral bending, respectively. Thirty-second wait periods were given following each load application. The flexibility parameters of neutral zone (NZ) and range of motion (ROM) were computed.

force to counterbalance the head weight or a head stop to restrict the head extension.

Flexibility Testing. Pure moments were applied to the occipital mount in four equal steps up to peak loads of 1.5 Nm, 3 Nm, and 1.5 Nm in flexion–extension, axial rotation, and lateral bending, respectively (Figure 3). To allow for viscoelastic creep, 30-second wait periods were given following each load application. Two preconditioning cycles were performed and data were recorded on the third loading cycle (Figure 4). Preliminary experimentation demonstrated that two load/unload cycles were adequate for preconditioning and that the kinematic data among subsequent cycles showed little change. From the resulting load displacement curves, the flexibility parameters of the neutral zone (NZ) and the range of motion (ROM) were determined for all intervertebral levels. The NZ is the region of high intervertebral laxity around the neutral posture, while the ROM is a measure of the entire range of intervertebral motion.[51]

Axial Rotation and Lateral Bending. Kinematic data during axial rotation and lateral bending flexibility tests were measured using the Optotrak three-dimensional motion measuring system (Northern Digital, Waterloo, Ontario, Canada) and a previous methodology.[27] The mean error for rotations within a 24° measurement range was −0.014° (SD 0.14°).[52]

Flexion–Extension. A custom-built loading apparatus, motion monitoring system, and customized software were integrated for automated flexion–extension flexibility testing. Sagittal kinematic motion data were recorded using a digital motion analysis camera (Fast Cam, Super 10k, model PS-110, Eastman Kodak Co., Rochester, NY) and analyzed using custom software. Single digital images were recorded at each motion step, and the centroids of the white flag markers were digitized, enabling computation of intervertebral angles. An experiment was performed to determine the total error of the system, which included errors of the measurement system and computation of the spinal flexibility parameters in response to applied loads. Six repeatability tests were performed with a 2-hour rest period between tests. The standard deviation of all the intervertebral motion measurements was 0.8°.

Following each flexibility test and before subsequent whiplash simulation, a 15-minute rest period was provided for specimen rehydration. During this period, the loading jig was removed and a tensile force was applied to C0 to counterbalance the weight of the occipital mount; the specimen was sprayed with 1% saline solution and wrapped with moistened gauze and plastic wrap.

Incremental Whiplash Simulation (3.5, 5, 6.5, and 8 *g*). Using a specially developed bench-top apparatus (Figure 5),[28] whiplash simulations were performed using the incremental trauma approach at nominal T1 horizontal maximum accelerations of 3.5, 5, 6.5, and 8 *g*. Before the whiplash simulations, a nominal 2 *g* simulation was performed to dynamically pre-

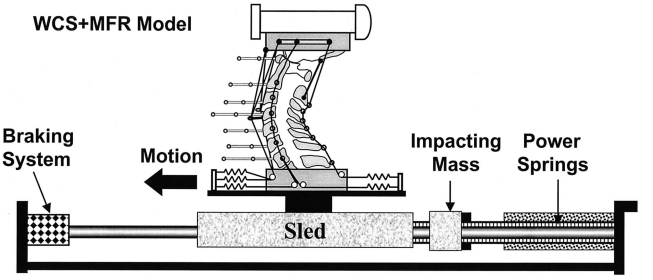

Figure 5. The whiplash apparatus and the WCS + MFR model. The main components of the whiplash apparatus included the sled mounted on linear bearings and an impacting system that consisted of power springs, a pneumatic piston, and an electromagnet release.

Table 1. Average (SD) Sagittal Neutral Zones (NZs) (°) as Measured by Flexibility Testing: Total (Flexion + Extension), Flexion and, Extension

	C0–C1	C1–C2	C2–C3	C3–C4	C4–C5	C5–C6	C6–C7	C7–T1
Total (flexion + extension) NZ								
2 g	22.9 (7.3)	10.9 (4.1)	6.3 (4.5)	7.8 (4.0)	12.5 (5.2)	11.8 (7.5)	12.8 (2.8)	5.8 (3.1)
3.5 g	22.9 (7.9)	11.1 (4.5)	6.1 (4.7)	8.4 (4.5)	13.4 (5.3)	12.6 (7.7)	13.1 (3.6)	6.4 (2.6)
5 g	23.6 (7.8)	11.9 (6.1)	7.9 (2.6)	8.9 (4.8)	13.4 (5.8)	13.6 (7.6)*	13.4 (4.2)	6.3 (3.0)
6.5 g	23.5 (7.4)	12.5 (4.6)	6.0 (3.9)	11.5 (5.8)	14.3 (4.9)*	13.9 (7.9)*	14.1 (4.3)	7.0 (2.0)†
8 g	23.8 (8.1)	11.1 (4.9)	6.8 (3.8)	12.5 (7.7)	14.7 (5.9)†	14.3 (8.4)*	14.8 (4.3)†	7.7 (3.0)*
Flexion NZ								
2 g	11.5 (3.6)	5.4 (2.0)	3.2 (2.2)	3.9 (2.0)	6.3 (2.6)	5.9 (3.8)	6.4 (1.4)	2.9 (1.6)
3.5 g	11.3 (3.1)	5.5 (3.2)	3.4 (2.4)	4.1 (2.4)	6.8 (2.5)	5.9 (4.4)	7.1 (1.7)	3.3 (1.4)
5 g	12.7 (3.7)	6.1 (3.9)	4.6 (1.8)	3.9 (2.5)	7.0 (2.9)	6.2 (4.3)	7.1 (1.6)	3.5 (1.8)
6.5 g	11.1 (3.7)	5.9 (3.6)	2.8 (1.5)	5.2 (2.2)	7.3 (3.2)†	6.5 (4.3)	7.3 (1.4)	4.0 (1.0)
8 g	11.3 (4.0)	4.8 (3.7)	3.9 (1.7)	3.7 (3.6)	7.2 (3.2)	6.6 (4.5)	7.4 (1.7)	3.9 (1.0)
Extension NZ								
2 g	11.5 (3.6)	5.4 (2.0)	3.2 (2.2)	3.9 (2.0)	6.3 (2.6)	5.9 (3.8)	6.4 (1.4)	2.9 (1.6)
3.5 g	11.6 (5.3)	5.6 (1.4)	2.8 (2.4)	4.3 (2.4)	6.6 (2.8)	6.7 (3.3)	6.0 (2.1)	3.1 (1.4)
5 g	10.8 (4.9)	5.8 (2.3)	3.2 (1.2)	5.0 (2.6)	6.4 (2.9)	7.4 (3.4)*	6.3 (2.7)	2.8 (1.5)
6.5 g	12. (5.8)	6.7 (1.7)	3.1 (3.2)	6.3 (5.5)	7.0 (3.7)	7.4 (3.7)*	6.8 (3.0)	3.0 (1.2)
8 g	12.5 (6.1)	6.3 (2.1)	2.9 (3.0)	8.8 (8.0)	7.5 (2.9)	7.7 (3.9)*	7.4 (3.2)	3.8 (2.1)†

Statistically significant increases with respect to the corresponding 2 g values: * $P < 0.01$; † $P < 0.05$.

condition the specimen. The major components of the whiplash apparatus included the sled, containing the rigidly attached T1 mount, and impacting and braking systems. The sled was mounted on horizontal linear bearings. The impacting system consisted of an impactor, rear of the sled, and power springs that were compressed by a pneumatic piston and activated by a computer controlled electromagnet release.

By configuring the power springs (stiffness and length) and the impactor, the T1 horizontal acceleration pulse was designed to represent the automobile acceleration profile of a real-life rear-end collision (Figure 5). The average T1 horizontal acceleration peaks actually measured during the whiplash simulations were 3.6, 4.7, 6.6, and 7.9 *g*, corresponding to the nominal maximum accelerations of 3.5, 5, 6.5, and 8 *g*, respectively. The average T1 horizontal acceleration pulse duration of 103.6 ms compared favorably with values measured during actual rear-end automobile collisions.

Data Analyses

Flexion–Extension Flexibility and Injury Potential. The flexibility data following the 2 *g* simulation was used as the baseline. A neutral position was defined in which each intervertebral joint was located midway between its total NZ from the 2 *g* flexibility test. To normalize the data, the injury potential was computed. It was defined as the relative percentage increase in a flexibility parameter following the 3.5, 5, 6.5, and 8 *g* whiplash simulations ($Flex_{Whiplash}$) compared with the corresponding value after the 2 *g* simulation ($Flex_{2g}$). Expressed mathematically, it was:

$$\text{Injury Potential (\%)} = (Flex_{Whiplash} - Flex_{2g}) \times 100/Flex_{2g}$$

Statistics. Single-factor, repeated-measures ANOVA and Bonferroni *post hoc* tests were used to determine significant changes ($P < 0.05$) in the multidirectional flexibility parameters. The injury threshold was the lowest T1 horizontal peak acceleration that caused a significant increase in either the NZ or ROM as compared with the corresponding 2 *g* value. The data were analyzed using Excel (Microsoft, Redmond, WA) and Minitab (Minitab Inc., State College, PA).

■ Results

The average 2 *g* dynamic baseline values for total sagittal (flexion plus extension) NZ and ROM varied among spinal levels (Tables 1 and 2). At the atlanto-occipital joint they were 22.9° and 26.9°, respectively, while the same at C7–T1 were 5.8° and 8.8°, respectively. The first significant increase ($P < 0.01$) over the 2 *g* baseline value was observed in the C5–C6 extension NZ following the peak T1 horizontal acceleration of 5 *g*. Thus, the injury threshold peak acceleration was 5 *g* and the mode of injury was extension. Following the 6.5 *g* whiplash simulation, significant increases were observed at C5–C6 and intervertebral levels above (1.8° in NZ and 1.3° in ROM at C4–C5) and below (1.2° in NZ and 1.4° in ROM at C7–T1). The 8 *g* simulation initiated significant increases at C0–C1 (1.8° in ROM), C3–C4 (6.0° in ROM), and C6–C7 (2.0° in NZ and 2.2° in ROM).

The injury potential parameters better illustrate the increased relative sensitivity of the NZ (Figure 6) as compared with the ROM (Figure 7) for determining the injury threshold acceleration and injury progression. The total NZ injury potentials (Figure 6A) showed earlier and greater significant increases ($P < 0.01$ or $P < 0.05$) than the total ROMs (Figure 7A). The total NZ and ROM injury potentials were divided into flexion and extension components to better understand the injury mechanism. In flexion, the only significant NZ increase was at C4–C5 following the 6.5 *g* simulation (Figure 6B), while no ROM increases were observed (Figure 7B). In extension, the NZ (Figure 6C) again showed more significant increases than the ROM (Figure 7C). At the injury threshold acceleration of 5 *g*, the C5–C6 extension NZ increased ($P < 0.01$) by 39.8% (Figure 6C), while no corresponding ROM increase was observed (Figure 7C). Following the 6.5 *g* whiplash simulation, the total NZ injury potential increases were greater than the corre-

Table 2. Average (SD) Sagittal Ranges of Motion (ROMs) (°) as Measured by Flexibility Testing: Total (Flexion + Extension), Flexion, and Extension

	C0–C1	C1–C2	C2–C3	C3–C4	C4–C5	C5–C6	C6–C7	C7–T1
Total (flexion + extension) ROM								
2 g	26.9 (7.2)	16.3 (3.6)	9.7 (5.5)	11.5 (4.5)	15.5 (5.9)	14.5 (7.7)	16.5 (3.2)	8.8 (3.2)
3.5 g	27.3 (7.8)	16.2 (4.1)	9.9 (5.3)	11.9 (4.2)	16.0 (5.5)	15.6 (7.9)	16.6 (3.9)	9.2 (2.5)
5 g	27.5 (7.9)	16.6 (4.5)	11.2 (3.8)	12.9 (4.4)	16.1 (6.0)	16.1 (8.1)	17.0 (4.6)	9.2 (3.0)
6.5 g	27.6 (7.8)	17.0 (3.9)	10.0 (4.6)	13.8 (6.7)	16.8 (5.5)†	16.4 (8.3)†	17.5 (4.6)	10.2 (2.4)†
8 g	28.7 (8.5)*	16.2 (4.0)	10.2 (4.5)	17.5 (8.7)†	17.7 (6.0)*	16.8 (9.0)*	18.7 (4.7)*	10.6 (2.5)*
Flexion ROM								
2 g	13.3 (3.6)	9.2 (1.9)	5.5 (2.9)	6.5 (2.6)	8.0 (3.2)	7.1 (4.2)	8.6 (1.4)	4.7 (1.8)
3.5 g	13.4 (3.0)	9.3 (2.7)	5.7 (3.2)	6.5 (2.2)	8.3 (2.9)	7.5 (4.5)	9.0 (1.2)	4.9 (1.4)
5 g	14.4 (3.6)	9.5 (2.8)	6.7 (2.8)	6.5 (2.1)	8.4 (3.3)	7.7 (4.7)	8.9 (1.4)	5.0 (2.0)
6.5 g	13.1 (3.3)	9.0 (3.0)	5.7 (1.8)	6.7 (1.7)	8.9 (3.5)	7.6 (4.3)	9.1 (1.1)	5.8 (1.6)
8 g	13.8 (3.7)	8.5 (3.2)	6.0 (1.7)	6.8 (3.2)	9.3 (3.2)	7.9 (4.7)	9.4 (1.8)	5.7 (0.7)
Extension ROM								
2 g	13.6 (3.7)	7.0 (1.9)	4.2 (2.6)	5.0 (2.1)	7.5 (2.7)	7.3 (3.7)	7.8 (2.3)	4.0 (1.6)
3.5 g	13.8 (5.2)	6.8 (1.5)	4.3 (2.1)	5.3 (2.5)	7.6 (2.8)	8.0 (3.7)	7.6 (3.1)	4.2 (1.3)
5 g	13.1 (4.8)	7.1 (1.9)	4.5 (1.2)	6.3 (2.6)	7.6 (2.9)	8.4 (3.5)	8.0 (3.4)	4.1 (1.5)
6.5 g	14.4 (6.1)	7.9 (1.4)	4.3 (3.3)	7.1 (7.1)	7.9 (2.6)	8.7 (4.1)	8.4 (3.8)	4.4 (1.4)
8 g	14.9 (6.6)	7.6 (1.6)	4.1 (3.3)	10.7 (8.3)	8.3 (3.1)	8.8 (4.5)	9.3 (3.8)†	4.8 (2.0)

Statistically significant increases with respect to the corresponding 2 g values: * $P < 0.01$; † $P < 0.05$.

sponding ROM increases: 19.3% in NZ and 11.2% in ROM at C4–C5, 20.8% in NZ and 16.4% in ROM at C5–C6, and 40.8% in NZ and 20.2% in ROM at C7–T1 (Figures 6A and 7A). Following the 8 *g* simulation, injury potential increases initiated at C0–C1 (5.8% in ROM), C3–C4 (35.5% in ROM), and C6–C7 (14.7% in NZ and 12.7% in ROM).

Results of the multidirectional flexibilities from intact to the final whiplash simulation demonstrated no significant increases in lateral bending or axial rotation (Tables 3 and 4).

■ Discussion

The chronic neck pain associated with rear-end collisions has been hypothesized to be associated with injury to the facet joints,[1–5] intervertebral disc,[6,7] spinal ligaments, spinal ganglions[8–10] in addition to psychosocial factors.[11–14] The present study identified the soft tissue injury threshold, based on the peak T1 horizontal acceleration, and the association between the impact magnitude and injury severity, using flexibility testing of a WCS model with muscle force replication (WCS + MFR) before and after simulated incremental whiplash at nominal peak accelerations of 3.5, 5, 6.5, and 8 *g*. Injury is the most important outcome of any whiplash simulation. We defined the injury as a significant increase in any of the flexibility parameters as compared to the corresponding 2 *g* dynamic baseline values. The injury threshold acceleration was the lowest T1 horizontal peak acceleration that caused a significant increase ($P < 0.05$) in the intervertebral flexibility. Our results demonstrated that the injury threshold peak acceleration of the current WCS + MFR model was 5 *g* as evidenced by a 39.8% increase ($P < 0.01$) in the C5–C6 extension NZ. There was no corresponding ROM increase following the 5 *g* simulation, indicating that the NZ was a more sensitive parameter than the ROM for detecting the injury threshold acceleration. At higher accelerations, injuries were observed throughout the middle and lower cervical spine.

Injuries to the lower cervical spine primarily resulted from intervertebral extension as significant increases in the extension NZs were observed at C5–C6 ($P < 0.01$) and C7–T1 ($P < 0.05$) following the 5 *g* and 8 *g* simulations, respectively, and the extension ROM ($P < 0.05$) at C6–C7 following the 8 *g* simulation. The only injury resulting from flexion was observed at C4–C5 following the 6.5 *g* simulation as indicated by an increase ($P < 0.05$) in the flexion NZ. No increases in flexion ROMs were observed.

Lateral bending and axial rotation flexibility testing was performed when the specimens were intact and following the final whiplash simulation. No changes in any of these flexibility parameters were found, which indicated that the sagittal plane loading resulting from the rear-impact whiplash simulation did not alter the elastic properties of the soft tissues that limit lateral and axial rotation motions. Thus, sagittal plane rear-impact whiplash caused only flexion–extension injuries.

The limitations of the current study must be considered before formulating conclusions regarding the injury threshold acceleration. The present study determined the osteoligamentous injury threshold of the cervical spine resulting from simulated whiplash and was not designed for determining the muscle injury. No attempt was made to replicate the innumerable intersegmental and global muscles or to model the active neuromuscular response in the WCS + MFR model. The MFR system provided stability to the WCS specimen and passive resistance to spinal motion following the impact, and thus, simulated the response of an unwarned subject. The T1 vertebra of the WCS + MFR model was fixed to the sled. Since the automobile acceleration profile during a rear-end collision is dependent on the energy absorbing characteristics of the bumper system, the injury threshold based on the T1 horizontal acceleration provided a universal param-

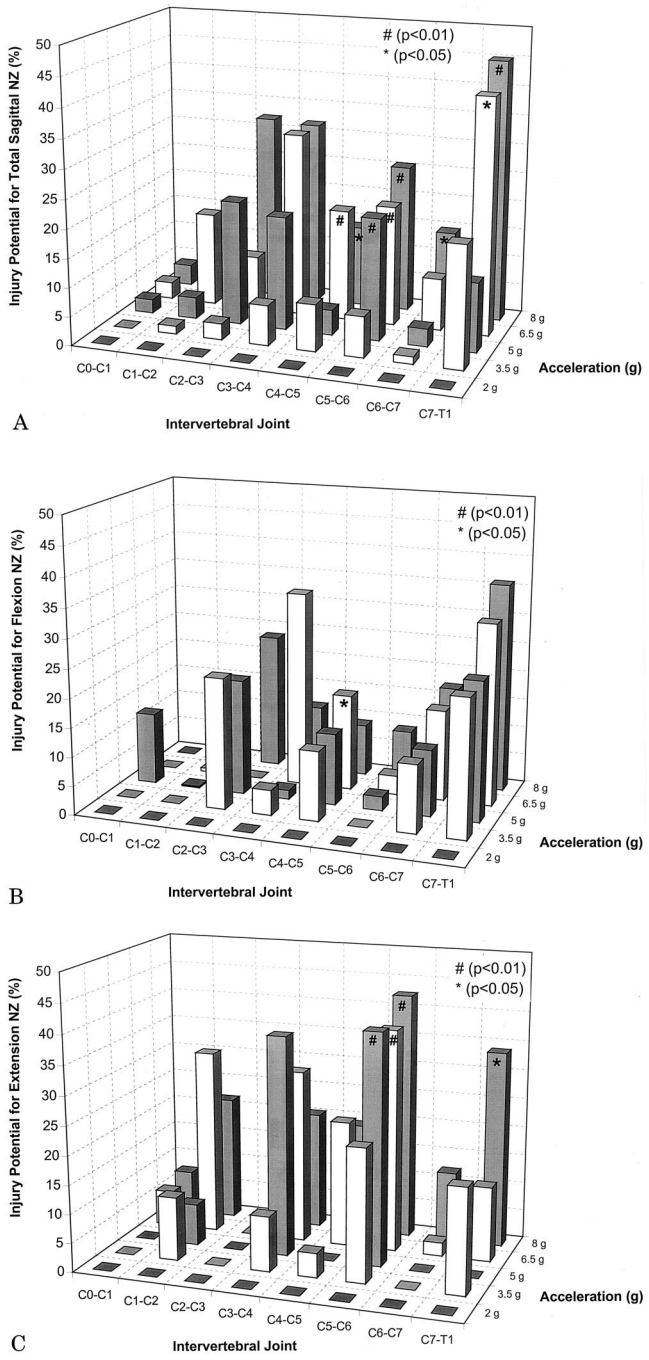

Figure 6. Injury potentials for sagittal neutral zones (NZs) for each intervertebral joint (C0–C1 to C7–T1) due to whiplash simulations at nominal T1 horizontal maximum accelerations of 3.5, 5, 6.5, and 8 *g*. Injury potentials represent the NZ percentage increases from corresponding 2 *g* values: total (flexion plus extension) (**A**), flexion (**B**), and extension (**C**). Statistical significances are indicated as follows: $\#P < 0.01$; $*P < 0.05$.

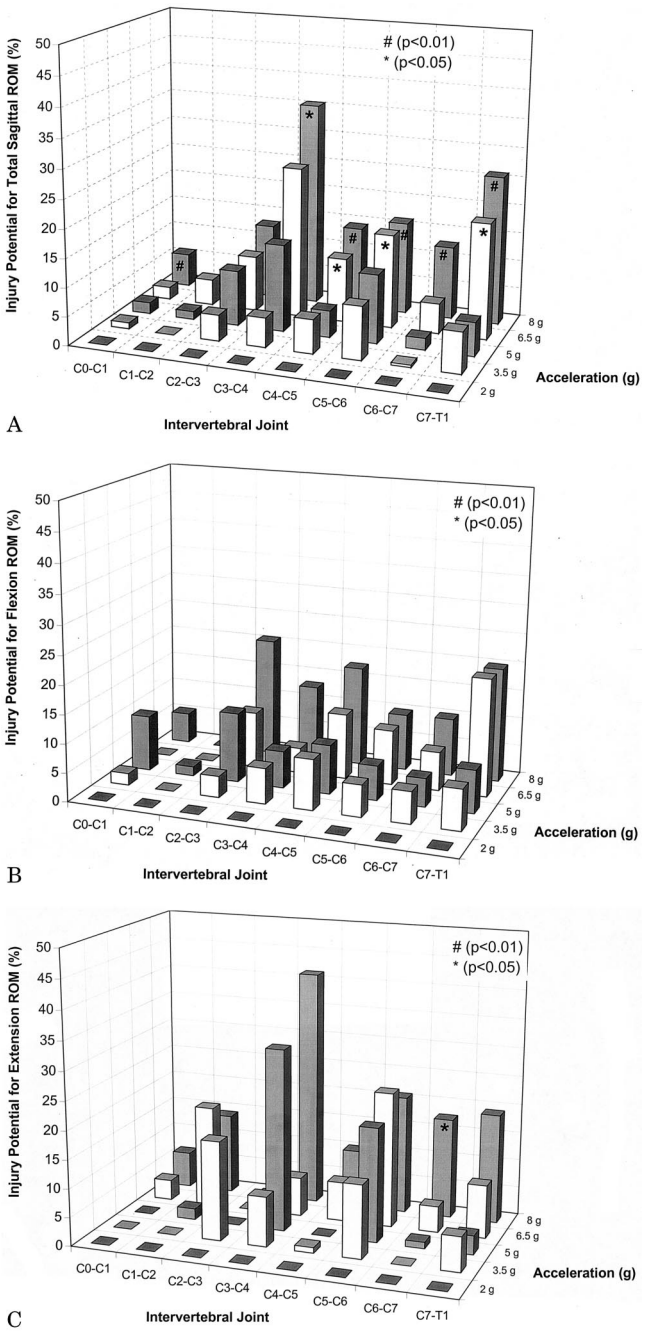

Figure 7. Injury potentials for sagittal ranges of motion (ROMs) for each intervertebral joint (C0–C1 to C7–T1) due to whiplash simulations at nominal T1 horizontal maximum accelerations of 3.5, 5, 6.5, and 8 *g*. Injury potentials represent the ROM percentage increases from corresponding 2 *g* values: total (flexion plus extension) (**A**), flexion (**B**), and extension (**C**). Statistical significances are indicated as follows: $\#P < 0.01$; $*P < 0.05$.

eter that could be used to develop injury prevention systems. The soft tissue injuries were quantified by the increases in the intervertebral joint laxity resulting from simulated whiplash and not *via* anatomic dissection since the subfailure soft tissue injuries were not visually identifiable. Provenzano *et al*[53] investigated the structural and cellular subfailure damage that resulted by stretching rat medial collateral ligaments (MCLs). They correlated the increased MCL strains with microscopically observable cellular damage and found that the MCL strains above the subfailure injury threshold caused increased MCL laxity. Additionally, cellular damage was noted at MCL strains significantly below the gross injury threshold.

Table 3. Average (SD) Neutral Zones (NZs) Measured by Multidirectional Flexibility Testing (°)

	Specimen State	C0–C1	C1–C2	C2–C3	C3–C4	C4–C5	C5–C6	C6–C7	C7–T1
Flexion + extension	Intact	21.7 (7.8)	9.6 (5.3)	4.5 (2.9)	5.8 (3.7)	10.3 (5.6)	10.9 (6.6)	9.7 (3.1)	3.6 (1.9)
	8 g	23.8 (8.1)*	11.1 (4.9)	6.8 (3.8)†	12.5 (7.7)*	14.7 (5.9)*	14.3 (8.4)*	14.8 (4.3)*	7.7 (3.0)*
Axial rotation (left + right)	Intact	2.2 (1.9)	47.6 (12.2)	2.2 (2.3)	1.6 (1.3)	3.5 (3.0)	2.4 (1.7)	1.4 (1.0)	1.2 (0.8)
	8 g	3.5 (2.3)	48.3 (14.0)	1.8 (1.9)	2.2 (2.2)	3.9 (2.8)	2.7 (2.2)	2.0 (1.1)	1.8 (0.9)
Lateral bending (left + right)	Intact	5.0 (2.4)	10.2 (8.8)	7.2 (3.7)	6.7 (5.5)	5.9 (3.5)	3.4 (2.0)	5.3 (2.9)	2.0 (0.5)
	8 g	5.1 (5.3)	10.6 (11.6)	8.8 (4.4)	7.9 (5.9)	5.8 (5.0)	4.2 (3.5)	6.0 (3.4)	1.4 (0.1)

Statistically significant increases with respect to the corresponding intact values: * $P < 0.01$; † $P < 0.05$.

To identify the soft tissue injury threshold acceleration, the incremental trauma approach was used. There are several advantages to this approach. The equivalency of the single and incremental trauma approaches has been validated for subfailure soft tissue injuries of porcine functional spine units,[54] subfailure and failure stretches of paired rabbit ligament preparations,[55] and the superiority of incremental trauma has also been demonstrated for experimental burst fracture studies.[56] In the former study, a high-speed axial compression trauma with a kinetic energy of 54.8 Nm was applied to the single trauma group. The incremental trauma group underwent traumas at kinetic energies of 13.7, 27.4, 41.1, and 54.8 Nm. Three-dimensional flexibility testing was performed on each functional spine unit before and after each trauma. Soft tissue subfailure injury was detected in both the single and incremental trauma groups; however, there were no statistical differences between the flexibility parameters of the two groups in any direction of motion, either before or after the final trauma. This well controlled high-speed trauma experiment serves as a validation of our incremental trauma approach, as simulated whiplash also results in soft tissue subfailure injuries. The incremental trauma approach in the rabbit ligament and burst fracture experiments produced similar results.[55,56]

The incremental trauma protocol has several important advantages as compared with the single trauma protocol for whiplash simulation. First, it allows for the injury threshold acceleration to be determined. The flexibility data after each incremental trauma are compared with the baseline data to determine the first significant increase, which identifies the injury threshold. Second, it allows for monitoring of the soft tissue injury progression. In contrast, the single trauma protocol has clear disadvantages. The acceleration chosen to produce the injury is defined *a priori*, and it may be either an underestimate, thus not producing clinically relevant injuries, or an overestimate resulting in fracture dislocations and complete ligament lesions. Consequently, to determine the injury threshold and injury progression using the single trauma protocol, several trauma groups are required and nonrepeated measures statistical analyses are performed. This requires many more scarce human cadaveric specimens in comparison with the incremental protocol. Thus, the incremental trauma approach of the current study is well justified.

In a previous study, Panjabi *et al*[27] evaluated the injury potential following simulated incremental whiplash using the WCS model without MFR. The injury threshold, based on the peak T1 horizontal acceleration, was found to be 4.5 *g* based on increases in the C5–C6 extension NZ and ROM. Additionally, the lower cervical spine had the greatest injury potentials, analogous to the results of the current study. However, there are some differences. On average, the percentage increases in sagittal flexibility parameters of the current model (45% peak NZ increase) tended to be lower than those reported by Panjabi *et al* (200% peak NZ increase).[27] There are two reasons for the differences. First, Panjabi *et al*[27] normalized the flexibility parameter increases with respect to the corresponding maximum physiologic values obtained during the intact flexibility tests. In the current study, we chose to dynamically precondition all specimens at the 2 *g* acceleration level and used the 2 *g* flexibility values as the dynamic baseline to normalize the data following each whiplash simulation. The 2 *g* value was chosen as the baseline as it was high enough to provide dynamic preconditioning to the soft tissues of the cervical spine but was well below the injury threshold acceleration.[5,31–39] Second, the MFR used in the current study most likely protected the soft tissues of the cervical spine during the simulated whiplash, especially at the

Table 4. Average (SD) Ranges of Motion (ROMs) Measured by Multidirectional Flexibility Testing (°)

	Specimen State	C0–C1	C1–C2	C2–C3	C3–C4	C4–C5	C5–C6	C6–C7	C7–T1
Flexion + extension	Intact	27.5 (7.7)	15.3 (4.2)	9.0 (4.0)	10.0 (4.5)	14.3 (5.5)	14.5 (8.0)	15.2 (3.1)	6.9 (2.4)
	8 g	28.7 (8.5)	16.2 (4.0)	10.2 (4.5)	17.5 (8.7)*	17.7 (6.0)*	16.8 (9.0)*	18.7 (4.7)*	10.6 (2.5)*
Axial rotation (left + right)	Intact	13.0 (5.5)	63.3 (13.0)	6.6 (4.8)	9.5 (4.9)	11.5 (3.8)	7.8 (4.1)	6.5 (2.3)	9.0 (5.1)
	8 g	11.5 (2.2)	63.6 (12.1)	6.6 (3.8)	12.5 (8.2)	12.5 (4.4)	8.6 (4.5)	7.0 (2.8)	9.9 (4.3)
Lateral bending (left + right)	Intact	7.7 (2.1)	11.6 (10.4)	9.7 (4.3)	8.6 (5.9)	8.1 (3.8)	4.9 (2.1)	6.8 (3.3)	3.9 (2.1)
	8 g	8.5 (4.7)	14.0 (12.1)	11.1 (5.2)	10.2 (6.8)	8.4 (5.6)	5.8 (4.1)	7.5 (3.4)	3.1 (0.2)

Statistically significant increases with respect to the corresponding intact values: * $P < 0.01$); † $P < 0.05$.

higher accelerations. The MFR system provided passive resistance to cervical spine motion following impact. The increases in the intervertebral flexibility parameters resulting from whiplash simulation of the WCS + MFR model with active neuromuscular response are currently unknown.

Chronic pain resulting from low-speed collisions may be explained by partial tears of the soft tissues, including anulus fibers, ligaments, and avascular cartilage. Because of poor blood supply, these tissues may not completely heal following injury, resulting in altered cervical spine kinematics that can lead to accelerated degenerative changes and clinical instability. WCS studies assist in determining the injury threshold acceleration and injury mechanisms of the passive soft tissues and have great potential to reduce future societal costs related to whiplash-associated disorders.

■ Conclusion

Biomechanical testing of the WCS before and after simulated whiplash demonstrated that the lower cervical spine had the greatest injury potential and the mode of injury was extension. The peak T1 horizontal acceleration of *5 g* was determined as the injury threshold acceleration. The first injuries occurred at the C5–C6 level, as indicated by increases in the extension neutral zone. At higher accelerations, the injuries spread to all intervertebral levels of the lower cervical spine from C4–C5 to C7–T1. The extension mode of injury may suggest that the onset of subfailure injuries of the anterior longitudinal ligament and anterior anulus fibers, in addition to facet joint impingement. Clinical evidence supports these injury mechanism hypotheses. The findings of the present study may be useful to the clinician for designing diagnostic and rehabilitation protocols and to the automotive engineer for designing improved occupant protection systems.

■ Key Points

- A newly developed biofidelic whole cervical spine model with muscle force replication was subjected to rear impacts of increasing severity.
- The soft tissue injury was defined as a significant increase ($P < 0.05$) in the intervertebral flexibility parameters of neutral zone or range of motion resulting from simulated whiplash.
- The injury threshold, based on the peak T1 horizontal acceleration, was *5 g* and the mode of injury was extension as evidenced by a 39.8% increase in the C5–C6 extension neutral zone. At higher accelerations, the injuries spread among the lower cervical spine.
- The neutral zone was a more sensitive parameter than the range of motion for determining the injury threshold.
- A rear-end collision is most likely to injure the lower cervical spine by intervertebral hyperextension.

References

1. Cusick JF, Pintar FA, Yoganandan N. Whiplash syndrome: kinematic factors influencing pain patterns. *Spine*. 2001;26:1252–1258.
2. Luan F, Yang KH, Deng B, et al. Qualitative analysis of neck kinematics during low-speed rear-end impact. *Clin Biomech*. 2000;15:649–657.
3. Panjabi MM, Cholewicki J, Nibu K, et al. Capsular ligament stretches during in vitro whiplash simulations. *J Spinal Disord*. 1998;11:227–232.
4. Winkelstein BA, Nightingale RW, Richardson WJ, et al. The cervical facet capsule and its role in whiplash injury: a biomechanical investigation. *Spine*. 2000;25:1238–1246.
5. Kaneoka K, Ono K, Inami S, et al. Motion analysis of cervical vertebrae during whiplash loading. *Spine*. 1999;24:763–769.
6. Jonsson H Jr, Cesarini K, Sahlstedt B, et al. Findings and outcome in whiplash-type neck distortions. *Spine*. 1994;19:2733–2743.
7. Pettersson K, Hildingsson C, Toolanen G, et al. Disc pathology after whiplash injury: a prospective magnetic resonance imaging and clinical investigation. *Spine*. 1997;22:283–287.
8. Eichberger A, Darok M, Steffan H, et al. Pressure measurements in the spinal canal of post-mortem human subjects during rear-end impact and correlation of results to the neck injury criterion. *Accid Anal Prev*. 2000;32:251–260.
9. Ortengren T, Hansson HA, Lovsund P, et al. Membrane leakage in spinal ganglion nerve cells induced by experimental whiplash extension motion: a study in pigs. *J Neurotrauma*. 1996;13:171–180.
10. Svensson MY, Bostrom O, Davidsson J, et al. Neck injuries in car collisions: a review covering a possible injury mechanism and the development of a new rear-impact dummy. *Accid Anal Prev*. 2000;32:167–175.
11. Schrader H, Obelieniene D, Bovim G, et al. Natural evolution of late whiplash syndrome outside the medicolegal context. *Lancet*. 1996;347:1207–1211.
12. Obelieniene D, Schrader H, Bovim G, et al. Pain after whiplash: a prospective controlled inception cohort study. *J Neurol Neurosurg Psychiatry*. 1999;66:279–283.
13. Ferrari R, Schrader H. The late whiplash syndrome: a biopsychosocial approach. *J Neurol Neurosurg Psychiatry*. 2001;70:722–726.
14. Partheni M, Constantoyannis C, Ferrari R, et al. A prospective cohort study of the outcome of acute whiplash injury in Greece. *Clin Exp Rheumatol*. 2000;18:67–70.
15. Lord SM, Barnsley L, Wallis BJ, et al. Percutaneous radio-frequency neurotomy for chronic cervical zygapophyseal-joint pain. *N Engl J Med*. 1996;335:1721–1726.
16. Lord SM, Barnsley L, Bogduk N. Percutaneous radiofrequency neurotomy in the treatment of cervical zygapophysial joint pain: a caution. *Neurosurgery*. 1995;36:732–739.
17. Lord SM, Barnsley L, Wallis BJ, et al. Chronic cervical zygapophysial joint pain after whiplash: a placebo-controlled prevalence study. *Spine*. 1996;21:1737–1744.
18. Barnsley L, Lord S, Bogduk N. Comparative local anaesthetic blocks in the diagnosis of cervical zygapophysial joint pain. *Pain*. 1993;55:99–106.
19. Barnsley L, Lord S, Bogduk N. Whiplash injury. *Pain*. 1994;58:283–307.
20. Barnsley L, Lord SM, Wallis BJ, et al. The prevalence of chronic cervical zygapophysial joint pain after whiplash. *Spine*. 1995;20:20–25.
21. Horst M. *Human head neck response in frontal, lateral and rear end impact loading: modelling and validation*, PhD thesis. Eindhoven, Eindhoven University of Technology, 2002.
22. Davidsson J. *Development of a mechanical model for rear impacts: evaluation of volunteer responses and validation of the model*, PhD thesis. Sweden: Chalmers University of Technology, 2000.
23. Yoganandan N, Cusick JF, Pintar FA, et al. Whiplash injury determination with conventional spine imaging and cryomicrotomy. *Spine*. 2001;26:2443–2448.
24. Yoganandan N, Pintar FA, Cusick JF. Biomechanical analyses of whiplash injuries using an experimental model. *Accid Anal Prev*. 2002;34:663–671.
25. Grauer JN, Panjabi MM, Cholewicki J, et al. Whiplash produces an S-shaped curvature of the neck with hyperextension at lower levels. *Spine*. 1997;22:2489–2494.
26. Panjabi MM, Cholewicki J, Nibu K, et al. Mechanism of whiplash injury. *Clin Biomech*. 1998;13:239–249.
27. Panjabi MM, Nibu K, Cholewicki J. Whiplash injuries and the potential for mechanical instability. *Eur Spine J*. 1998;7:484–492.
28. Panjabi MM, Cholewicki J, Nibu K, et al. Simulation of whiplash trauma using whole cervical spine specimens. *Spine*. 1998;23:17–24.
29. Stemper BD, Yoganandan N, Pintar FA. Intervertebral rotations as a function of rear impact loading. *Biomed Sci Instrum*. 2002;38:227–231.
30. Cholewicki J, Panjabi MM, Nibu K, et al. Head kinematics during in vitro whiplash simulation. *Accid Anal Prev*. 1998;30:469–479.

31. Szabo TJ, Welcher JB. *Human subject kinematics and electromyographic activity during low speed rear impacts* [Paper No. 962432]. Society of Automotive Engineers, 1996.
32. Scott MW, McConnell WE, Guzman HM, et al. *Comparison of human and ATD head kinematics during low-speed rear-end impacts* [Paper No. 930094]. Society of Automotive Engineers, 1993.
33. Ono K, Kaneoka K, Wittek A, et al. *Cervical injury mechanism based on the analysis of human cervical vertebral motion and head-neck-torso kinematics during low speed rear impacts* [Paper No. 973340]. Society of Automotive Engineers, 1997.
34. McConnell WE, Howard RP, Poppel JV, et al. *Human head and neck kinematics after low velocity rear-end impacts: understanding 'whiplash'* [Paper No. 952724]. Society of Automotive Engineers, 1995.
35. McConnell WE, Howard RP, Guzman HM, et al. *Analysis of human test subject kinematic responses to low velocity rear end impacts* [Paper No. 930889]. Society of Automotive Engineers, 1993.
36. Matsushita T, Sato TB, Hirabayashi K, et al. *X-ray study of the human neck motion due to head inertia loading* [Paper No. 942208]. Society of Automotive Engineers, 1994.
37. Kumar S, Narayan Y, Amell T. An electromyographic study of low-velocity rear-end impacts. *Spine*. 2002;27:1044–1055.
38. Kaneoka K, Ono K, Inami S, et al. Human cervical spine kinematics during whiplash loading. *International Conference on New Frontiers in Biomechanical Engineering*. Tokyo, Japan, 1997:265–268.
39. Brault JR, Siegmund GP, Wheeler JB. Cervical muscle response during whiplash: evidence of a lengthening muscle contraction. *Clin Biomech*. 2000;15: 426–435.
40. Patwardhan AG, Havey RM, Meade KP, et al. A follower load increases the load-carrying capacity of the lumbar spine in compression. *Spine*. 1999;24: 1003–1009.
41. Rohlmann A, Neller S, Claes L, et al. Influence of a follower load on intradiscal pressure and intersegmental rotation of the lumbar spine. *Spine*. 2001; 26:E557–E561.
42. Quint U, Wilke HJ, Shirazi-Adl A, et al. Importance of the intersegmental trunk muscles for the stability of the lumbar spine: a biomechanical study in vitro. *Spine*. 1998;23:1937–1945.
43. Quint U, Wilke HJ, Loer F, et al. Laminectomy and functional impairment of the lumbar spine: the importance of muscle forces in flexible and rigid instrumented stabilization—a biomechanical study in vitro. *Eur Spine J*. 1998; 7:229–238.
44. Wilke HJ, Wolf S, Claes LE, et al. Stability increase of the lumbar spine with different muscle groups: a biomechanical in vitro study. *Spine*. 1995;20:192–198.
45. Patwardhan AG, Havey RM, Ghanayem AJ, et al. Load-carrying capacity of the human cervical spine in compression is increased under a follower load. *Spine*. 2000;25:1548–1554.
46. Bernhardt P, Wilke HJ, Wenger KH, et al. Multiple muscle force simulation in axial rotation of the cervical spine. *Clin Biomech*. 1999;14:32–40.
47. Kettler A, Hartwig E, Schultheiss M, et al. Mechanically simulated muscle forces strongly stabilize intact and injured upper cervical spine specimens. *J Biomech*. 2002;35:339–346.
48. Panjabi MM, Miura T, Cripton PA, et al. Development of a system for in vitro neck muscle force replication in whole cervical spine experiments. *Spine*. 2001;26:2214–2219.
49. Braakman R, Penning L. *Injuries of the Cervical Spine*. Netherlands: Excerpta Media, 1971.
50. McKenzie JA, Williams JF. The dynamic behaviour of the head and cervical spine during 'whiplash.' *J Biomech*. 1971;4:477–490.
51. Panjabi MM. The stabilizing system of the spine: II. Neutral zone and instability hypothesis. *J Spinal Disord*. 1992;5:390–396.
52. Kifune M, Panjabi MM, Arand M, et al. Fracture pattern and instability of thoracolumbar injuries. *Eur Spine J*. 1995;4:98–103.
53. Provenzano PP, Heisey D, Hayashi K, et al. Subfailure damage in ligament: a structural and cellular evaluation. *J Appl Physiol*. 2002;92:362–371.
54. Atlas OK, Dodds SD, Panjabi MM. Single and incremental trauma models: a biomechanical assessment of spinal instability. *Eur Spine J*. 2002;12:205–210.
55. Panjabi MM, Huang RC, Cholewicki J. Equivalence of single and incremental subfailure stretches of rabbit anterior cruciate ligament. *J Orthop Res*. 2000;18:841–848.
56. Panjabi MM, Hoffman H, Kato Y, et al. Superiority of incremental trauma approach in experimental burst fracture studies. *Clin Biomech*. 2000;15:73–78.